

SUPPLEMENTARY INFORMATION

Patterned conductive nanostructures from reversible self- assemble of 1D coordination polymer

Denis Gentili, Gonzalo Givaja, Rubén Mas-Ballesté, Mohamad R. Azani, Arian Shehu, Francesca Leonardi, Eva Mateo-Martí, Pierpaolo Greco, Félix Zamora* and Massimiliano Cavallini*

Materials and Methods

$[\text{Pt}_2(n\text{BuCS}_2)_4\text{I}]_n$ polymer and its precursors were synthesized according to methods published elsewhere.¹ All reagents were purchased from Aldrich and used as received. Electronic absorption spectra were recorded on an Agilent 8452 diode array spectrophotometer over a 190–1100 nm range in 0.2 cm quartz cuvettes thermostatted by a Unisoku cryostat. ¹H NMR spectra in CD_2Cl_2 were recorded on a Bruker AMX-300 spectrometer, using TMS as external reference.

Lithographic methods

Solvents: The solutions were prepared using dichloromethane (Aldrich, anhydrous, $\geq 99.8\%$) and tetrahydrofuran (Aldrich, anhydrous, $\geq 99.9\%$).

Stamps: The elastomeric polydimethylsiloxane stamps (PDMS, Sylgard 184, Dow Corning) stamps were prepared by replica molding of a blank Compact Disk for parallel lines (periodicity of 1.5 μm , width at half height 500 nm and 220 nm deep), a photolithographic master for interdigitated comb-like microstructures and for OFET microelectrodes (two parallel lines with width at half height 500 μm and distance of 70 μm , provided by SCRIBA Nanotecnologie S.r.l.). PDMS stamps were cured for 6 h at 60°C, then peeled off and washed in pure ethanol for one hour.

Substrates: Si wafers (n-type doped) with 200 nm thermally grown SiO_2 layer, borosilicate glass with 250 nm gold layer (ArrandeeTM, Germany), and microscope glass slides. All substrates were sonicated in electronic-grade water (milli-pure quality, 2 min), in acetone (Aldrich chromatography quality, 2 min), then in 2-propanol (Aldrich spectroscopic grade quality, 2 min), and blown dry in N_2 .

MIMIC: the stamp grooves placed in contact with the substrate (silicon oxide, glass, and gold surfaces) form capillary channels and $[\text{Pt}_2(n\text{BuCS}_2)_4\text{I}]_n$ solution, poured at the open end of the stamp, flows into microchannels by capillary forces (Figure 1a). After the complete evaporation of the solvent, the stamp is gently removed leaving the micro and nanostructures on the surface.

LCW: the stamp is gently placed in contact with a film of $[\text{Pt}_2(n\text{BuCS}_2)_4\text{I}]_n$ solution spread on the substrate and the capillary forces pin the solution to the stamp protrusions, giving rise to an array of

menisci (Figure 1b). After the complete evaporation of the solvent, the stamp is gently removed leaving the micro and nanostructures on the surface.

Characterization: Optical micrographs were recorded with a Nikon i-80 microscope equipped with epilluminator, dark-field and cross polars using 50X objective. AFM images were recorded with a commercial AFM (NT-MDT, Moscow, Russia) operating in semi-contact mode in ambient condition. Si₃N₄ cantilevers, with typical curvature radius of a tip 10 nm were used. Image analysis was done using the open source SPM software Gwyddion-www.gwyddion.net. SEM images were collected using an S-4000 (Hitachi) instrument.

Scanning Electron Microscopy: The Scanning Electron Microscopy (SEM) images were obtained with a ZEISS 1530 SEM equipped with a Schottky emitter and operating at 10 keV. The instrument was equipped with an Energy Dispersive X-Ray Spectrometer (EDX) for X-Ray microanalysis, and two different Secondary Electrons (SE) detectors, the InLens (IL) and the Everhart-Thornley detectors (ETD). The IL detector collected a secondary electrons component (the so-called SE1) generated by the primary incident beam in a small region around the beam impinging point, and for this reason it shows an higher sensibility to surface morphology. The ETD collects the complete SE spectrum, the SE1 component, but also the SE generated by the back scattered electrons (BSE) emitted by the specimen (SE2) and the SE generated by the BSE colliding with the chamber of the instrument (SE3). In addition ETD acts also as a BSE detector with a rather low efficiency. Therefore the detected signal shows a reduced sensitivity to the local surface morphology, but a higher sensitivity to the density and/or compositional variations.

Electrical characterization: The mobility in the saturation regime (μ_{sat}) was calculated using the equation $I_{\text{DS}} = (W/2L)C_i\mu_{\text{sat}}(V_{\text{G}}-V_{\text{th}})^2$, where C_i is the capacitance of the insulating SiO₂ layer and V_{th} is the threshold voltage extracted from the square root of the drain current ($I_{\text{DS}}^{0.5}$) versus gate voltage (V_{G}) characteristics for a fixed drain voltage (V_{DS}). The OFET devices were measured in atmospheric conditions.

X-ray Photoelectron Spectroscopy (XPS)

XPS analyses of the samples were carried out in an ultrahigh vacuum chamber equipped with a hemispherical electron analyzer, and using an Al K α X-ray source (1486.6 eV). The base pressure in the

chamber was 5×10^{-10} mbar, and the experiments were performed at room temperature. The following core level peaks were recorded under the same experimental conditions: O(1s), C(1s), S(2p), I(3d), Pt(4f) and Au(4f). The pass energy applied for taking the overview sample was 30 eV, while 20 eV pass energy was applied for the fine analysis of the core level spectra. The core-level binding energies were calibrated against the binding energy of the Au(4f_{7/2}) peak set to 84.0 eV for gold surface sample; with this calibration, the carbon peak attributed to hydrocarbon contamination was measured at 284.6 eV. The peak deconvolution in different components was shaped, after background subtraction, as a convolution of Lorentzian and Gaussian curves. Lorentzian and Gaussian widths of 0.1 and 1 eV, respectively, common for all the components, were used.

XPS analysis has been performed in order to obtain chemical information related to the [Pt₂(nBuCS₂)₄I]_n before and after surface deposition. In a wide scan XPS overview spectra of a compacted [Pt₂(nBuCS₂)₄I]_n pellet, the following atomic species can be identified: C, S, I and Pt. The same atomic species have been identified after the adsorption of [Pt₂(nBuCS₂)₄I]_n on gold surface. Therefore, there is a good agreement between solid compound and after adsorption on gold surface (Table S1).

In order to obtain the chemical state of Pt element in the [Pt₂(nBuCS₂)₄I]_n compound, selected Pt(4f) energy region from 66 to 82 eV was individually scanned. Figure S6 shows the core-level spectra of the Pt(4f). The binding energy of Pt (4f_{7/2}) peak shows two components at 72.7 and 74.2 eV assigned to Pt²⁺ and to Pt³⁺, respectively². In both cases (pellet and adsorption on gold surface of the [Pt₂(nBuCS₂)₄I]_n) the Pt(4f) peak shows two components and the percentage of the two components are Pt²⁺ (76%) and to Pt³⁺ (24%).

Table S1. Binding energies (eV) and with of the peaks^{[a], [b]} from the XPS data of [Pt₂(nBuCS₂)₄I]_n on bulk and patterned on gold surfaces.

	Pt ²⁺	Pt ³⁺	Pt ²⁺	Pt ³⁺
	4f _{7/2}	4f _{7/2}	4f _{5/2}	4f _{5/2}
Bulk	72.32 (1.9)	74.17 (2.0)	75.66	77.51
Stripes	72.68 (1.8)	74.22 (1.3)	76.02	77.56

^[a] Full width at half-maximum values for peaks are given in parentheses. ^[b] Values corrected against the Au 4f_{7/2} peak set at 84.0 eV.

Polarization Modulation Reflection Absorption Infrared Spectroscopy (PM-RAIRS)

The PM-RAIRS spectra were recorded on a commercial NICOLET Nexus spectrometer. The external beam was focused on the sample, with a mirror, at an optimal incident angle of 80°. The incident beam was modulated between p and s polarizations with a ZnSe grid polarizer and a ZnSe photoelastic modulator (HINDS Instruments, PEM 90, modulation frequency = 37 kHz). The light reflected at the sample was then focused on a nitrogen-cooled mercury-cadmium-telluride detector. All spectra were recorded at 8 cm⁻¹ resolution by co-adding 128 scans. The PM-RAIRS signal is given by the differential reflectivity ($\Delta R/R$) $(R_p - R_s)/(R_p + R_s)$.^{3,4}

Figure S7 shows RAIRS spectra of MMX compound immobilized on gold surface from solution. The infrared spectra contain intense absorptive features indicative that MMX compound has been successfully adsorbed on the gold surface.

A RAIR spectrum shows several bands in the region from 3000 to 2850 cm⁻¹, which corresponds to CH₂ and CH₃ asymmetric and symmetric stretching modes, which identify that CH₂ and CH₃ groups are present in the [Pt₂(*n*BuCS₂)₄I]_n compound. Other vibrations related with these functional groups appear in the spectra as: the δ (CH₂) scissoring vibration band at 1457 cm⁻¹, CH₃ deformation modes δ (CH₃)_{sym} (symmetrical bending) at 1361 cm⁻¹ and δ (CH₃)_{asym} at 1450 cm⁻¹.

Usually, the stretching frequencies of dithiocarboxylate complexes of Ni(II) and Zn(II) are observed between 900 and 1100 cm⁻¹.^{5,6} In our case the most intense broad band in the spectra appears at 1111-1043 cm⁻¹. This intense absorption in the 1050–1100 cm⁻¹ region has been previously assigned to the CS₂⁻ group asymmetric stretching vibration, the corresponding symmetric stretching vibration is located below 850 cm⁻¹, it is not possible to identify in our spectra range. The presence of CS₂⁻ group means that the ligand bridges two metal atoms (Pt) through two sulfur atoms, each sulfur atom coordinates to one of two metal atoms in this case, respectively and the two C–S bonds are completely delocalized.

RAIRS comparisons spectra between dust compound and after compound adsorption on gold surface have been performed in order to further understand MMX interaction on the surface. While dust infrared spectra shows only vibration band at 1080 cm⁻¹ region previously assigned to the CS₂⁻ group, in good agreement with the crystallographic data for the MMX compound, that indicate almost coincident C-S bond lengths, confirming the equivalency of both sulphur atoms. On the other hand, once [Pt₂(*n*BuCS₂)₄I]_n has been adsorbed on the gold surface RAIRS spectra shows two extra intense bands at 1264 and 1043 cm⁻¹, which cannot be assigned to any other infrared vibration than C=S and C-S stretching vibrations respectively, meaning that adsorption process on the surface could take place via the sulphur atom, this suggestion is in a good agreement with the well-known S-Au affinity, therefore interaction through the CS₂⁻ group on the gold surface make the two sulphur in-equivalence (C=S and C-S).

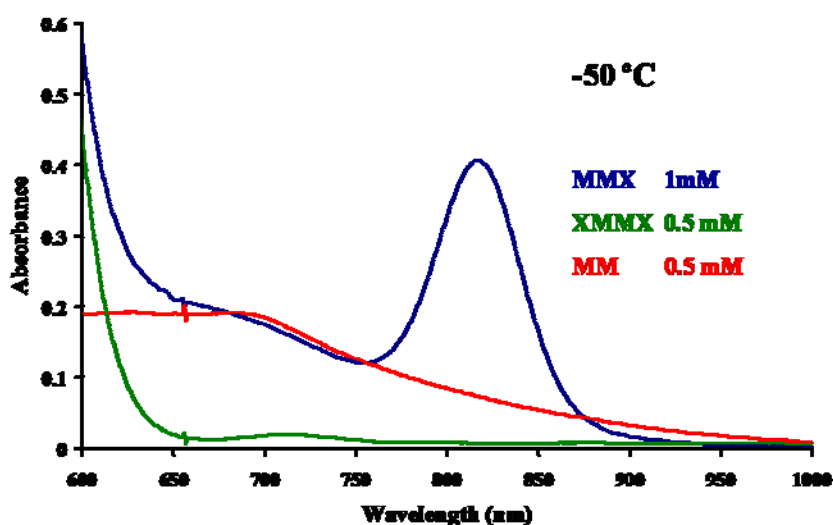


Figure S1. UV-vis spectrum of a 1 mM solution of $[\text{Pt}_2(n\text{BuCS}_2)_4\text{I}]_n$ in CH_2Cl_2 , compared with UV-vis spectra of 0.5 mM solutions of $[\text{Pt}_2(n\text{BuCS}_2)_4]$ and $[\text{Pt}_2(n\text{BuCS}_2)_4\text{I}_2]$ in CH_2Cl_2 . All data was taken at $-50\text{ }^\circ\text{C}$. Spectrum of $[\text{Pt}_2(n\text{BuCS}_2)_4\text{I}_2]$ does not show significant variations with respect to the data observed at room temperature. $[\text{Pt}_2(n\text{BuCS}_2)_4]$ solution at low temperature presents the appearance of a new absorption in the range of 600-700 nm due to $\text{MM}\cdots\text{MM}$ association. In the MMX spectrum at $-50\text{ }^\circ\text{C}$ two new absorptions appear: One at 600-700 nm attributed to $\text{MM}\cdots\text{MM}$ assembly and another one at 820 nm assigned to $\text{MM}\cdots\text{XMMX}$ association. Absorption at 600-700 nm in the 1 mM MMX solution is lower than the observed in 0.5 mM solution of MM because part of the MM present in solution goes to $\text{MM}\cdots\text{XMMX}$ assemblies.

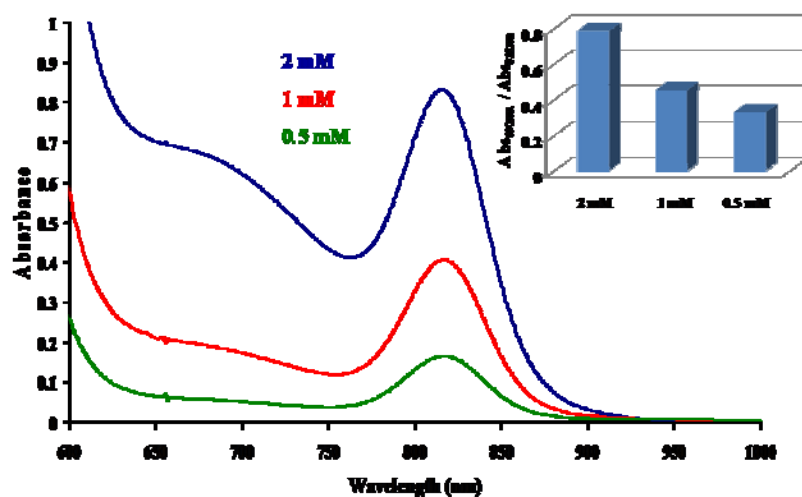


Figure S2. UV-vis spectra of 2 mM, 1 mM and 0.5 mM solutions of $[\text{Pt}_2(n\text{BuCS}_2)_4\text{I}]_n$ in CH_2Cl_2 measured at $-50\text{ }^\circ\text{C}$. The ratio between $\text{MM}\cdots\text{MM}$ and $\text{MM}\cdots\text{XMMX}$ assemblies depends on the concentration. At higher concentrations the relative amount of $\text{MM}\cdots\text{MM}$ suprastructures increases.

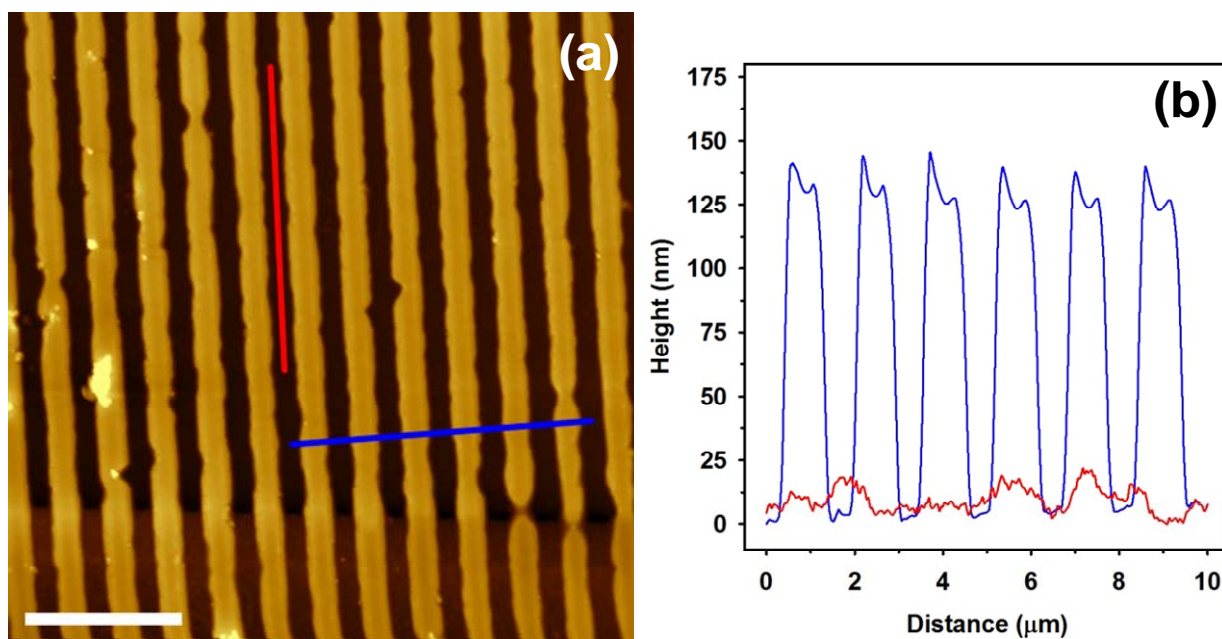


Figure S3. a) AFM morphology (scale bar = 5 μm), and b) AFM profiles of $[\text{Pt}_2(\text{nBuCS}_2)_4\text{I}]_n$ wires patterned on gold electrodes (LCW, parallel lines, 2 mg/mL in CH_2Cl_2).

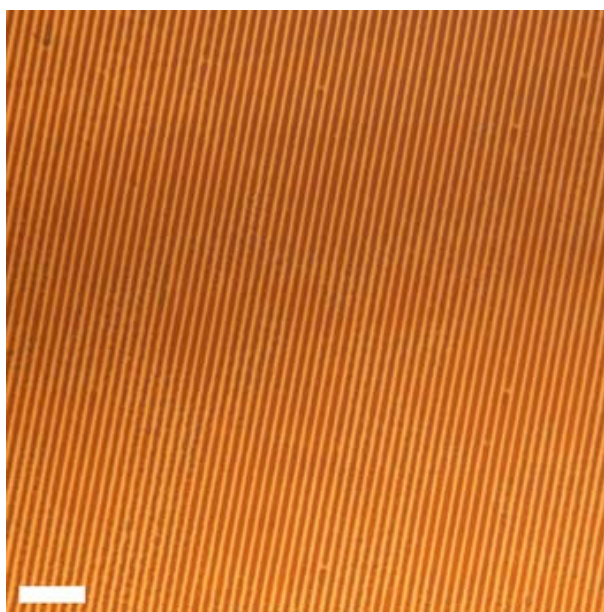


Figure S4. Optical microscopy (scale bar = 10 μm) of $[\text{Pt}_2(\text{nBuCS}_2)_4\text{I}]_n$ wires patterned on gold surface (LCW, parallel lines, 1 mg/mL in CH_2Cl_2).

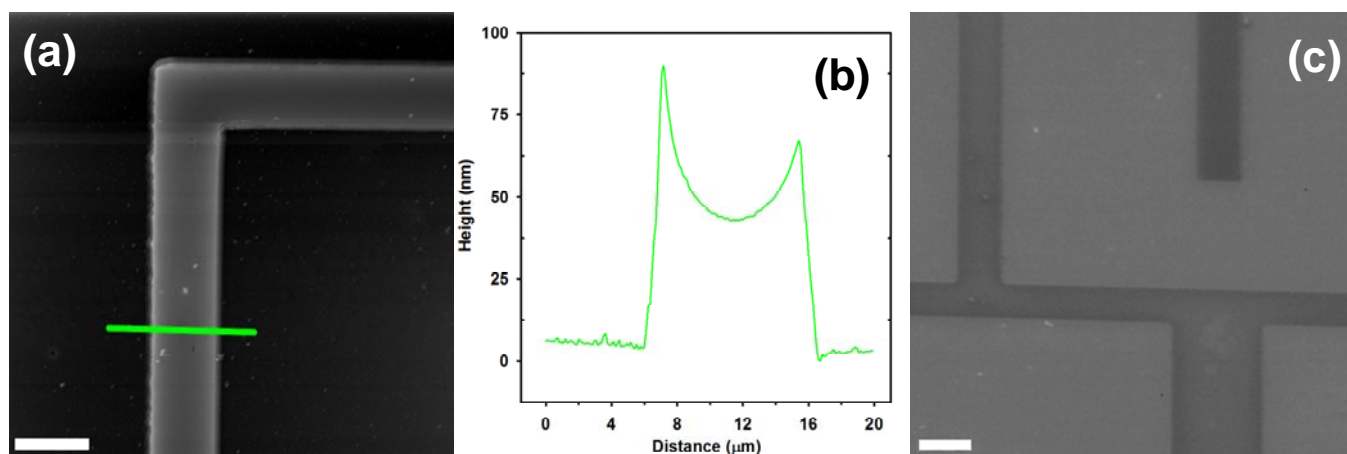


Figure S5. a) AFM image (scale bar = 10 μm), b) AFM profile, and c) SEM (scale bar = 10 μm) of $[\text{Pt}_2(\text{nBuCS}_2)_4\text{I}]_n$ pattern on silicon oxide (LCW, interdigitated comb-like, 2 mg/mL in CH_2Cl_2).

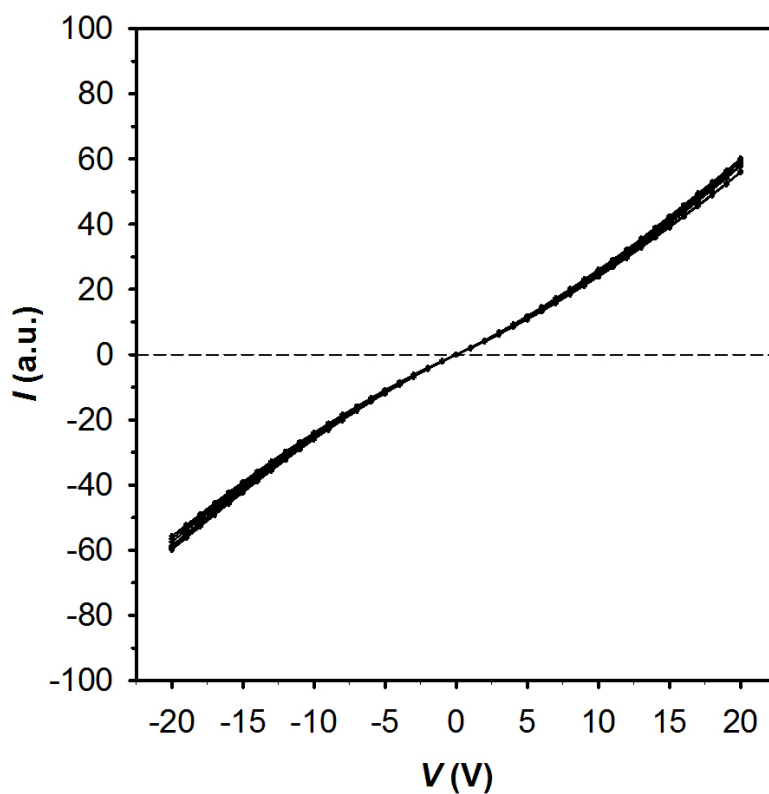


Figure S6. Current vs voltage characteristic upon the application of 10 cycles on wires patterned on gold electrodes.

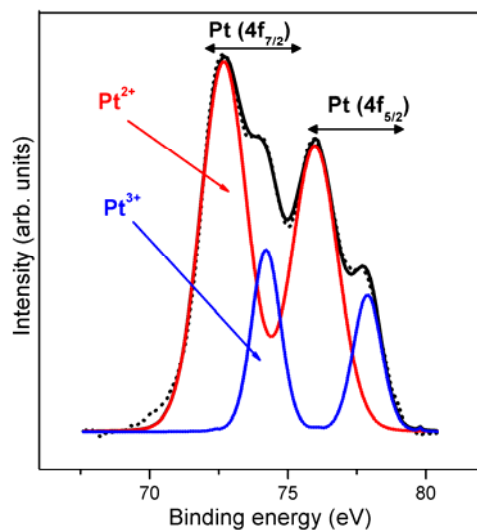


Figure S7. XPS core-level peak of Pt ($4f_{7/2}$ and $4f_{5/2}$) from $[\text{Pt}_2(n\text{BuCS}_2)_4\text{I}]_n$ on gold surface. The binding energies values of the two components of the Pt $4f_{7/2}$ peak are 72.7 eV (red line) and 74.2 eV (blue line) assigned to Pt^{2+} and Pt^{3+} , respectively.

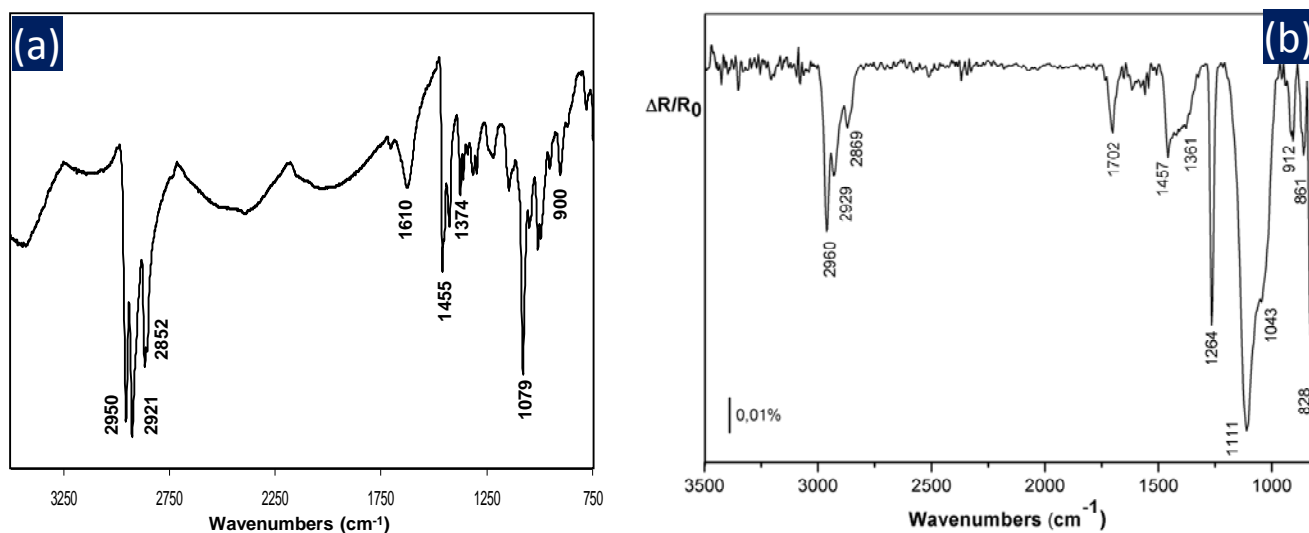


Figure S8. FTIR (a) in PM-RAIRS spectra after adsorption of $[\text{Pt}_2(n\text{BuCS}_2)_4\text{I}]_n$ on gold surfaces from solution.

References

1. Mitsumi, M. *et al.*, Valence-ordering structures and magnetic behavior of metallic MMX chain compounds, *Angew. Chem. Int. Ed.* **41**, 2767-2771 (2002).
2. Mitsumi, M. *et al.*, Metallic behavior and periodical valence ordering in a MMX chain compound, Pt-2(EtCS₂)(4)I, *J. Am. Chem. Soc.* **123**, 11179-11192 (2001).
3. Barner, B.J., Green, M.J., Saez, E.I., and Corn, R.M., Polarization Modulation Fourier-Transform Infrared Reflectance Measurements of Thin-Films and Monolayers at Metal-Surfaces Utilizing Real-Time Sampling Electronics, *Anal. Chem.* **63**, 55-60 (1991).
4. Buffeteau, T., Desbat, B., and Turlet, J.M., Polarization Modulation Ft-Ir Spectroscopy of Surfaces and Ultra-Thin Films - Experimental Procedure and Quantitative-Analysis, *Appl. Spectrosc.* **45** (3), 380-389 (1991).
5. Shankaranarayana, M. and Patel, C.C., Infrared Spectra and Structures of Xanthates and Dixanthogens, *Can. J. Chem. Rev. Can. Chim.* **39**, 1633-1636 (1961).
6. Burke, J.M. and Fackler, J.P., Vibrational-Spectra of Dithioaryl Acid Complexes of Nickel(Ii), Palladium(Ii), Platinum(Ii), and Zinc(Ii), and Their Sulfur Addition Products - X-Ray Crystal-Structure of Dimer of Bis(Dithiocumato)Platinum(Ii)-a Material with a 2.87ure of Dimer of Bis(Dithiocumato)Plaa Metal-Metal Bond, *Inorg. Chem.* **11**, 3000-3008 (1972).